JOURNAL OF MATERIALS SCIENCE 21 (1986) 2705–2710

Effect of cutting speed and tool rake angle on residual stress distribution in machining 2024-T351 aluminium alloy – unlubricated conditions

S. JEELANI, S. BISWAS
School of Engineering and Architecture, Tuskegee University, Tuskegee, Alabama 36088, USA
R. NATARAJAN
Department of Mechanical Engineering, University of Illinois at Chicago, Chicago, Illinois 60680, USA

The residual stress distribution in the machining of 2024-T351 aluminium alloy was measured using an electrolytic etching technique. Ring-shape specimens were machined under unlubricated orthogonal conditions with high-speed steel tools having rake angles of 10, 15, 20 and 25° at cutting speeds ranging between 0.5 and 1.25 m sec^{-1}. The results of the investigation show that the residual stresses are compressive at the machined surface and decrease with depth beneath the machined surface. The maximum (near-surface) residual stress and the depth of the severely stressed region increase with an increase in the cutting speed. There seems to be little change in the residual stress distribution due to a change in the rake angle. The results are interpreted in terms of the variations in the amount of surface-region deformation produced by changes in cutting conditions.

1. Introduction

The process of machining metal is complex. The type of surface generated depends on several variables: the work and tool materials, tool geometry, cutting speed, feed, the presence or absence of a lubricant in the cutting region, etc. Previous investigations have shown that in the machining of metals a damaged surface region is produced that is quite different from the bulk of the material [1–5]. The damage in the surface region consists of plastic deformation, which is a result of the interaction between the nose region of the tool and the machined surface of the workpiece. The nose region includes the cutting edge and the land and rake face of the tool. The machined surface of the material contains residual stress, the magnitude and nature of which depend on the parameters mentioned above. The geometric defects in the surface consists of grooves parallel to the direction of relative tool motion, fine-scale chatter marks, cavities, surface roughness and other stress risers. The presence of a lubricant is the cutting region usually results in a considerable reduction in the surface and subsurface damage [6, 7].

One of the most important characteristics associated with surface-region alteration in components machined from high-strength materials is the residual stress distribution, because it can greatly affect material stability and resistance to deformation. In general, the stability and resistance to deformation of a material and its fatigue life are increased by the presence of compressive residual stresses, and decreased by the presence of tensile residual stresses.

The purpose of the present investigation was to determine by the method of stress relief the effects of changes in cutting speed and tool rake angle on the residual stress distribution in rings of 2024-T351 aluminium alloy machined under dry, orthogonal conditions. This method is based on the fact that sectioning and the removal of layers of material from the machined surface of a ring relieve a portion of the residual stresses and disturb the existing conditions of equilibrium. This causes the remaining stresses to redistribute themselves and attain a new equilibrium by producing a change in curvature of the ring. Measurements of the changes in curvature can then be used to compute the residual stress.

2. Experimental work

2.1. Workpiece and tool

In this investigation 2024-T351 aluminium alloy was used as the work material: the chemical composition and mechanical properties of this alloy are given elsewhere [8]. This material was selected because of its wide application as an engineering structural material in industry. It has high strength and good strength-to-weight ratio and is therefore extensively used in weight-sensitive situations, especially in modern aircraft and ship components. The work material was received in the form of extruded seamless tubing. Ring-shaped specimens were cut as shown in Fig. 1.

0022–2461/86 $03.00 + .12

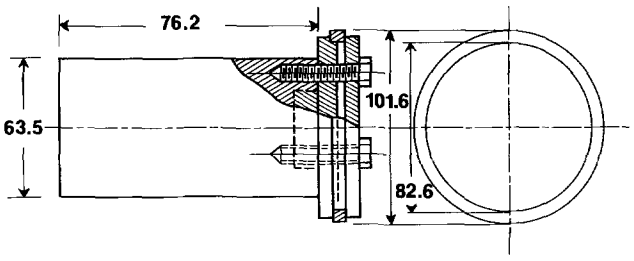

Figure 1 Workpiece and mandrel. Dimensions in mm.

TABLE I Summary of cutting conditions

Cutting speed ($m\,sec^{-1}$)	0.50, 0.75, 1.00, 1.25
Feed ($mm\,rev^{-1}$)	0.254
Rake angle (deg)	10, 15, 20, 25
Clearance angle (deg)	5
Width of cut (mm)	6.35
Tool wear land (mm)	0.000
Lubricant/coolant	None
Tool material	High-speed steel

The workpiece was clamped to a mandrel as shown in Fig. 1 while machining. The material selected for this work was high-speed steel.

A special tool fixture was designed to hold the cutting tools while grinding, in order to make certain that all the tools had the same rake and clearance angles. The tool faces were first rough-ground with a 60-grit silicon carbide grinding wheel. A 120-grit silicon carbide wheel was then used to achieve a fine surface on the rake and flank faces. A water-soluble oil was used as lubricant in the grinding of the tools.

2.2. Cutting tests

The tests were conducted over a wide range of cutting conditions under unlubricated orthogonal conditions. In orthogonal machining the direction of tool motion (feed) is perpendicular to the axis of rotation of the workpiece and the cutting edge is perpendicular to the direction of relative work–tool motion. Fig. 2 illustrates the orthogonal cutting process. A summary of the cutting conditions used in this investigation is shown in Table I.

Once steady-state cutting was established, the cutting action was suddenly stopped and the workpiece was removed from the mandrel. A diametral line was then scribed across the side surface of the ring and the outside diameter was determined accurately. This was then cut into two parts so that one part extended approximately 10 mm beyond the diametral line at each of its ends. The outside diameter of this ring was measured along the diametral line, and the change in diameter produced by cutting (because of the partial relief of residual stresses) was determined. The three unmachined surfaces of larger portions of semi-circular rings were coated with a non-conducting corrosion-resistant paint.

2.3. Experimental set-up

Fig. 3 shows the apparatus used for the determination of residual stress distribution. The electro-etching tank was constructed from 6.35 mm thick plexiglass. Entry and exit ports were provided so that a continuous supply of electrolyte (2% aqueous solution of sodium chloride) can be maintained. In this way electrolyte contamination was reduced to a minimum.

The test specimen (anode) and the stainless steel ring (cathode) were held in a fixture such that the distance between them was constant over the entire specimen length. The specimen-holding fixture was attached to the bottom of the electrolytic etching tank. The cathode was permanently attached to the fixture while the anode was held between two expandable plastic pieces which could accomodate specimens of various cross-sectional dimensions.

A power supply unit was arranged to provide a d.c. supply of constant current up to 4 A. A laser beam was used for measurement of the angular deflection of the specimen, as shown in Fig. 4. This was positioned at the level of a plane mirror attached to the top of the specimen. The mirror was attached to the specimen in such a way that the length of the mirror was perpendicular to the diametral axis of the specimen. So, initially, when the beam of the laser was incident on the mirror it reflected back to the origin of the beam. As electrolysis continued the mirror changed its position with a change in deflection of the ring, so that the beam of light reflected back to another position on the scale. The reading on the scale was carefully noted. Etching was carried out until there was no further change in deflection.

The initial thickness and the final thickness after electro-etching of the specimen were measured by a micrometer. Assuming the etching process to be linear, the thickness of the layer removed at any interval of time during electro-etching was obtained by calculating the average removal rate from the initial and final thickness of the specimen.

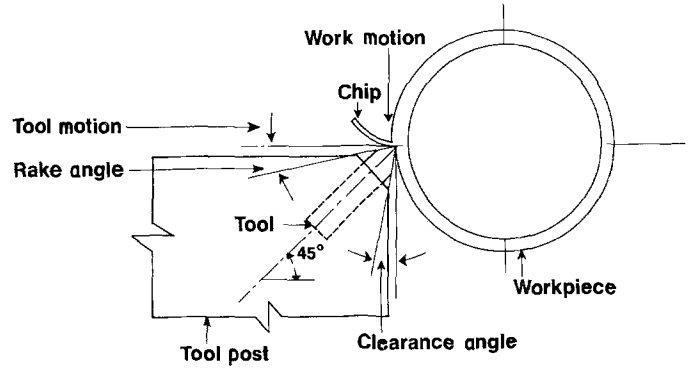

Figure 2 Orthogonal machining.

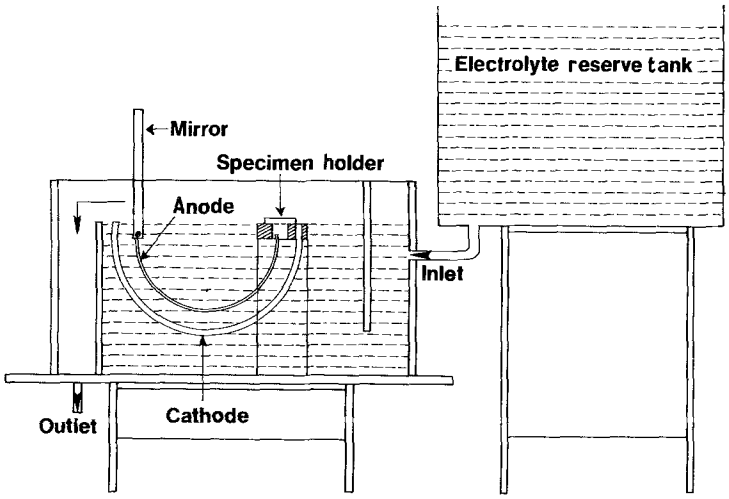

Figure 3 Electrolytic etching apparatus.

3. Determination of residual stress distribution

The second theorem of Castigliano is used to determine the residual stress distribution in a machined ring as a function of depth beneath the machined surface. For the experimental deflection–electrochemical etching technique used in the present work, relief of residual stresses in a given layer (n) occurs through removal of that layer by etching ($\sigma_{1,n}$), removal of previous layers by etching ($\sigma_{2,n}$), and the initial cutting of the ring ($\sigma_{3,n}$). The actual residual stress is, therefore, the sum of these three components.

A semicircular section of a machined ring containing residual stress is shown in Fig. 5. One end of the ring is fixed in a rigid support and the other end is attached to a first surface mirror. If a layer of thickness, dt, is removed from the outer surface of the ring the free end (the one attached to the mirror) will deflect. The mirror as a body will experience translational (δ) and rotational (ψ) motion. The laser beam will deflect only due to the rotation of the mirror. The rotation of the mirror is given by

$$\psi = -\frac{6\sigma_{1,n}\pi R\,dt}{Et^2} \tag{1}$$

where R is the radius of the ring, t is the thickness of the ring and E is the modulus of elasticity of the material. The width of the ring remains constant throughout the etching process and, therefore, does not appear in the expression for the rotation (ψ) of the ring. Equation 1 may be rewritten as

$$\sigma_{1,n} = -\frac{Et^2\psi}{6\pi R\,dt} \tag{2}$$

If L represents the perpendicular distance between the mirror and the screen in Fig. 4, and Y the distance moved on the screen,

$$\sigma_{1,n} = -\frac{Et^2 Y}{12\pi RL\,dt} \tag{3}$$

Stress relief due to removal of previous layers and the initial cutting is given by

$$\sigma_{2,n} = A\{d\Delta_{n-1}[4t_0 - 4(n-1)\,dt] - 2\Delta t(d\Delta_{n-2} + d\Delta_{n-3} + \ldots + d\Delta_0)\} \tag{4}$$

where $A = E/6\pi RL$, and

$$\sigma_{3,n} = -\frac{d\Delta DE}{2R^2}\left(Z - \frac{t_0}{2}\right) \tag{5}$$

respectively, where $d\Delta_n$ is the deflection of the ring because of removal of the nth layer, $d\Delta D$ is the change in the diameter of the ring because of cutting and t_0 is the initial thickness of the ring. The remaining thickness of the ring (Z) is given by

$$Z = t_0 - n\,dt \tag{6}$$

Fig. 6 explains the terms used in the above equations.

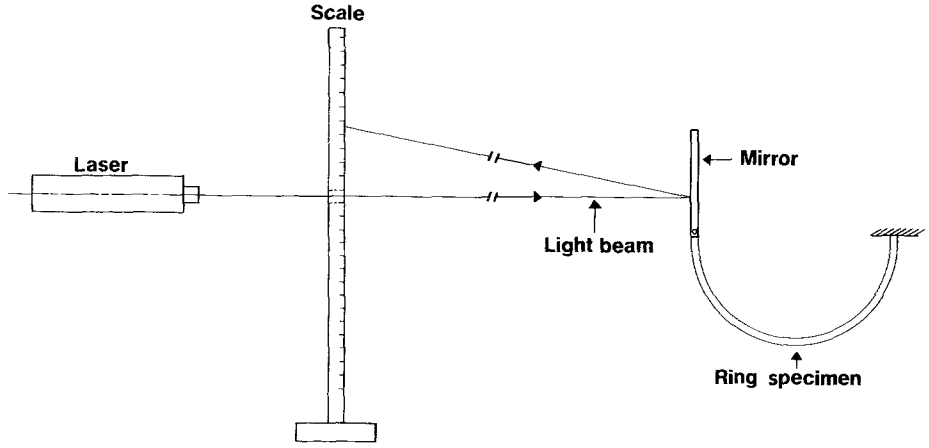

Figure 4 Measurement of deflection.

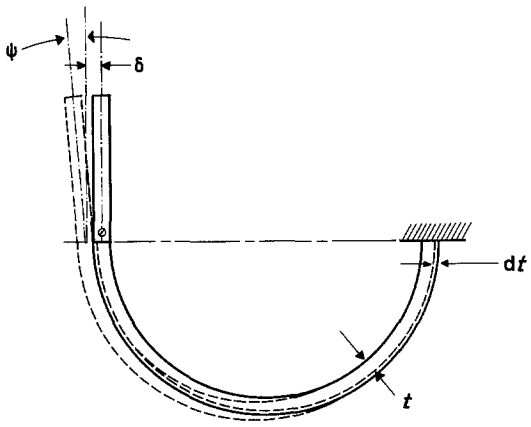

Figure 5 Displacement of the free end of the half-ring.

The total stress in the nth layer is given by

$$\sigma_{T,n} = \sigma_{1,n} + \sigma_{2,n} + \sigma_{3,n} \quad (7)$$

A detailed development of Equations 1 to 7 may be found elsewhere [9]. It may be pointed out here that $\sigma_{T,N}$ is the tangential (or hoop) stress. Other components (radial and axial) are considered to be negligible.

4. Results

A considerable amount of data was generated on the residual stress distribution in 2024-T351 aluminium alloy, which was machined over a wide range of cutting conditions. In the following only selected data representative of the results in general are presented. Complete data may be found in [9].

Figs 7 and 8 show the residual stress distribution in the surface region of workpieces machined with a sharp cutting tool having rake angles of 10 and 20°, respectively, at cutting speeds ranging from 0.5 to 1.25 m sec^{-1}. It can be seen that the maximum (near-surface) residual stress is high (compressive) and decreases in magnitude rapidly with an increase in depth beneath the machined surface. Complete analysis of the data showed that the residual stresses continued to decrease in magnitude across the section, becoming tensile on the inside surface of the ring. similar results were obtained when machining was carried out with tools having rake angles of 15 and 25°. It is, of course, not possible to obtain the actual residual stress at the machined surface, because of the incremental manner in which layers are removed from the surface by etching and the procedures that are used to calculate the residual stresses.

Figs 9 and 10 show the residual stress distribution in the surface region of the workpiece machined at cutting speeds of 0.5 and 1.25 m sec^{-1}, respectively, with sharp tools having rake angles of 10, 15 and 20, and 25°. It can be seen that the near-surface residual stress is high (compressive) and decreases in magnitude with an increase in depth beneath the machined surface. Changes in the rake angle seem to have no effect on the residual stress distribution for all the cutting speed used in this investigation.

In general, the results also show that an increase in the cutting speed produces an increase in the depth of the severely stressed surface region.

5. Discussion

Residual stresses in the surface regions of machined workpieces are generated principally by two factors, namely plastic deformation and the volume of material associated with thermal gradients and metal lurgical alterations in structure. The problem is complicated further because often these factors may act synergistically.

Chip formation takes place by a process of shear in a zone known as the "primary deformation zone" that extends from the tool cutting edge to the junction between the surfaces of the chip and workpiece. If the mode of deformation (flow) of material in the zone is such that it extends below the nose of the cutting tool then clearly it can induce plastic deformation in the surface region of the workpiece. Deformation may be enhanced if adhesion develops between the tool wear land and the freshly machined workpiece surface. Heat generated by this plastic deformation and heat conducted from the primary and secondary deformation zones can produce a significant increase in temperature in the surface region.

For a given material the mode of deformation (flow) in the primary deformation zone and the type of

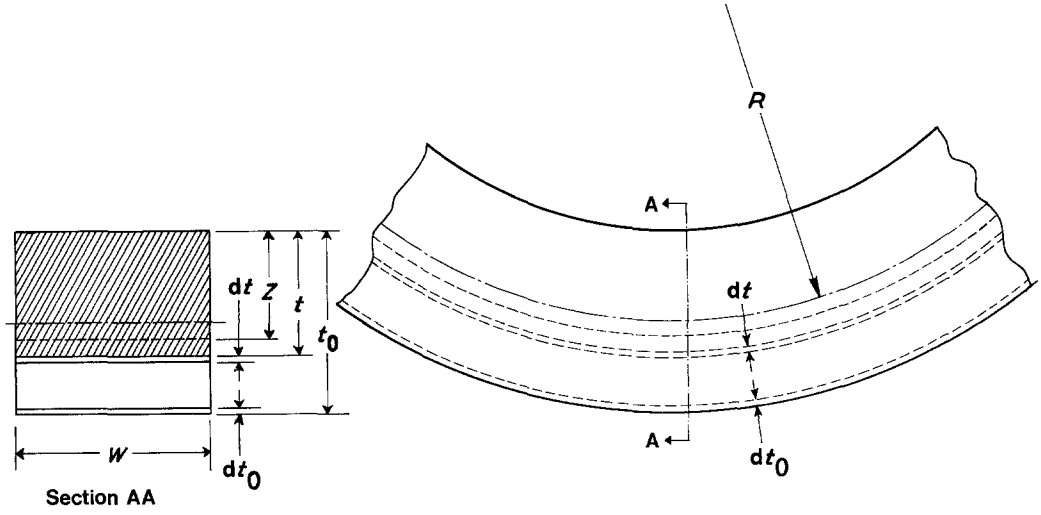

Figure 6 Section of the ring.

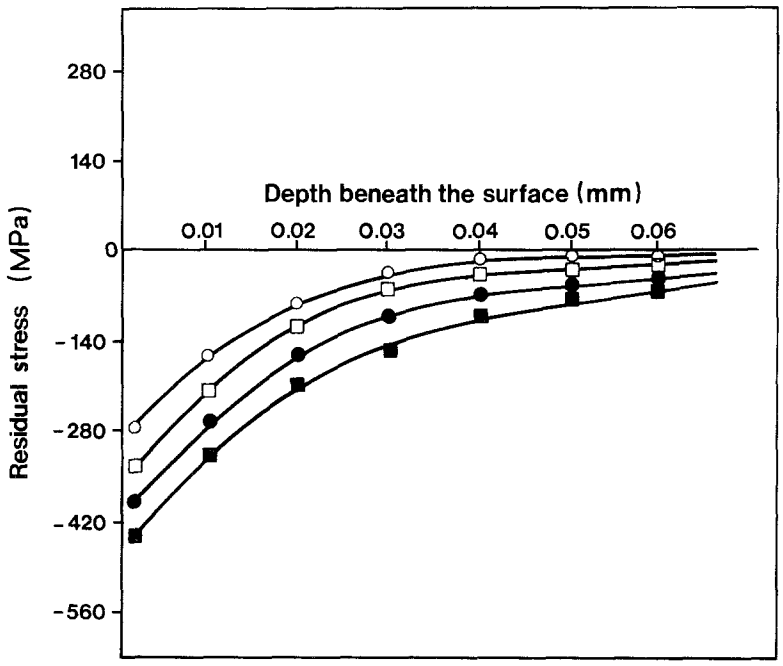

Figure 7 Residual stress distribution in 2024-T351 aluminium machined with a tool having a rake angle of + 10°. Cutting speed (○) 0.50, (□) 0.75, (●) 1.00, (■) 1.25 m sec^{-1}.

chip produced depend on the existing conditions of strain, strain rate and temperature that are themselves determined largely by the cutting speed and tool geometry. Adhesion at the tool land–workpiece interface depends primarily on the energy of adhesion which is, in turn, a function of the mechanical and physical properties of the metallic pair. The important physical quantities that may determine the final stress distribution appear to be the strain and temperature distributions generated in the surface region during machining.

In machining 2024-T351 aluminium alloy, it was observed that the chip formation process was partially discontinuous at low cutting speeds with a sharp tool, which produced fracture and cavity formation in the surface region [10]. It is suggested that protrusion of the primary deformation zone below the nose of the tool produces a ploughing action that leads to surface region deformation, accompanied by work-hardening and the generation of residual stress. At low cutting speeds, temperatures in the surface region are insufficient to overcome the work-hardening produced by plastic deformation. It is believed, however, that some relief of residual stress occurs because of the surface-region fracture. Thus, the maximum (near-surface) residual stress remains low. It was also observed that an increase in cutting speed produced a change in the chip formation process from partially discontinuous to continuous, with an increase in the cutting and thrust components of the resultant tool force. The increase in the thrust component led, in turn, to an increase in both the depth of plastic deformation below the surface region and the extent of surface work-hardening. Again, it appears that the temperature rise in the surface region of the workpiece is insufficient to overcome work-hardening, even at high

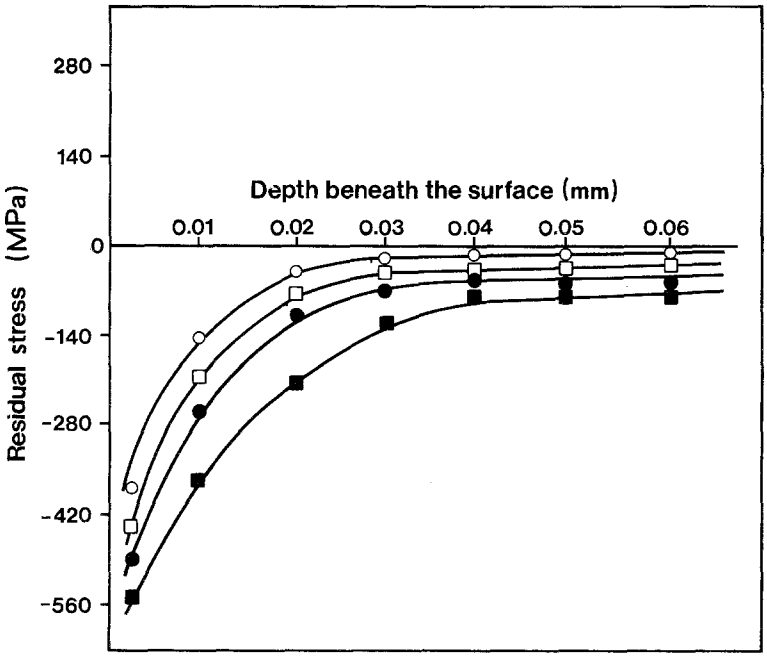

Figure 8 Residual stress distribution in 2024-T351 aluminium machined with a tool having a rake angle of + 20°. Cutting speed (○) 0.50, (□) 0.75, (●) 1.00, (■) 1.25 m sec^{-1}.

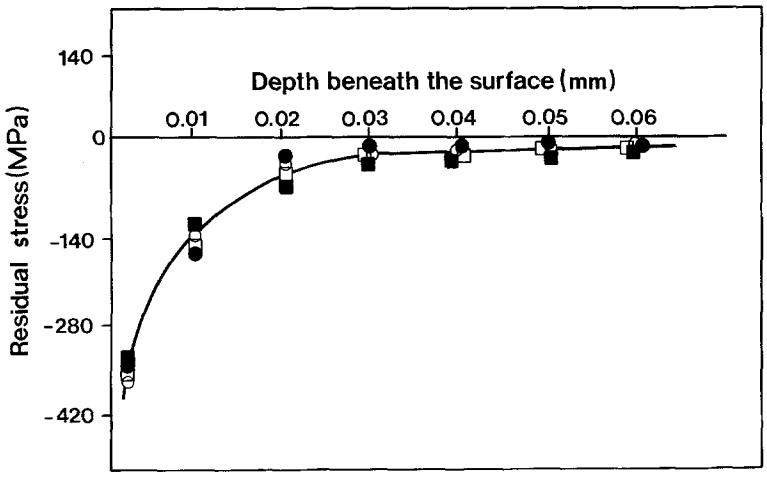

Figure 9 Residual stress distribution in 2024-T351 aluminium machined at a cutting speed of 0.5 m sec^{-1}. Rake angle (○) 10, (□) 15, (●) 20, (■) 25°.

cutting speeds. It is believed that the increase in surface-region deformation brought about by an increase in cutting speed leads to an increase in both the maximum (near-surface) residual stress and the depth of the severely stressed layer.

It was found that an increase in tool rake angle at a given cutting speed produced little increase in the cutting and thrust components of the resultant tool force; there was therefore, no change in either the depth of plastic deformation in the surface region or the extent of surface-region work-hardening.

6. Conclusions

1. Compressive residual stresses are generated in the surface region of ring-shaped workpieces of 2024-T351 aluminium alloy machined under dry, unlubricated conditions.

2. The residual stress is maximum at the surface and decreases in magnitude with an increase in the depth beneath the surface.

3. The magnitude of the maximum (near-surface) residual stress and the thickness of the severely stressed surface region increases with an increase in the cutting speed at a given tool rake angle.

4. The magnitude of the maximum (near-surface) residual stress and the thickness of the severely stressed surface region are not affected by an increase or decrease in the tool rake angle at a given cutting speed.

5. The results can be interpreted in terms of variations in the amount of surface-region deformation produced by variations in both the tool forces and in the type of chip produced with changes in cutting conditions.

References

1. S. JEELANI, PhD thesis, North Carolina State University (1975).
2. J. A. BAILEY and S. JEELANI, *SME Trans.* (1974) 174.
3. *Idem, Wear* **36**(2) (1976) 199.
4. J. A. BAILEY, S. JEELANI and S. E. BECKER, *ASME J. Engng. Ind.* **98**(3) (1976) 999.
5. J. A. BAILEY and S. JEELANI, *Wear* **72** (1981) 237.
6. J. A. BAILEY, *ibid.* **42** (1977) 297.
7. *Idem, ibid.* **4** (1977) 371.
8. M. MUSIAL, MS thesis, Tuskegee Institute, Alabama (1983).
9. S. BISWAS, MS thesis, Tuskegee Institute, Alabama (1985).
10. S. JEELANI and M. MUSIAL, *J. Mater. Sci.* **21** (1986) 155.

Received 15 May
and accepted 26 September 1985

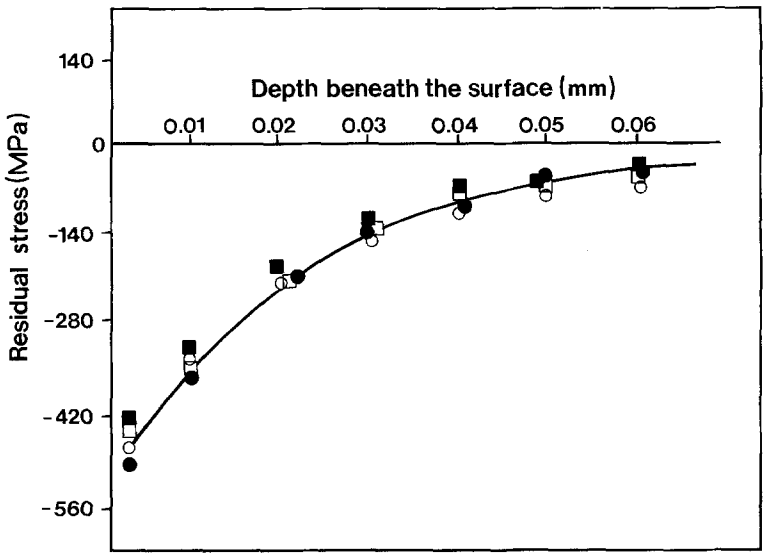

Figure 10 Residual stress distribution in 2024-T351 aluminium machined at a cutting speed of 1.25 m sec^{-1}. Rake angle (○) 10, (□) 15, (●) 20, (■) 25°.